International Journal of Science and Research Archive
eISSN: 2582-8185
Cross Ref DOI: 10.30574/ijsra
Journal homepage: https://ijsra.net/

(RESEARCH ARTICLE)

Check for updates

X-ray diffraction pattern profiling and sustainable production of crystalline nano-cellulose acetate from waste cotton linter: Crystallite size analysis insights

Nusrat Zahan [1], Md. Mazedul Haque Sachchu [2, 3, *], Mohshin Maola [1], Md. Tauhidul Islam [1], Md. Ralin Islam [1, 3], Anik Biswas [1], Tumpa Rani Kar [4], Md. Ashraful Alam [5] and Md. Shamsul Alam [1, *]

[1] *Department of Applied Chemistry and Chemical Engineering (ACCE), Islamic University, Kushtia-7003, Bangladesh.*
[2] *Department of Chemical Engineering, Bangladesh University of Engineering and Technology (BUET), Dhaka, 1000, Bangladesh.*
[3] *Retexhub Limited, House No-23, Road-3/C, Sector-9, Uttara Model Town, Dhaka-1230, Bangladesh.*
[4] *Department of Chemistry, Jahangirnagar University, Savar, Dhaka-1342, Bangladesh.*
[5] *Institute of Glass and Ceramic Research and Testing (IGCRT), Bangladesh Council of Scientific and Industrial Research (BCSIR), Dhanmondi, Dhaka-1205, Bangladesh.*

International Journal of Science and Research Archive, 2026, 19(01), 464-477

Publication history: Received on 24 March 2026; revised on 07 April 2026; accepted on 10 April 2026

Article DOI: https://doi.org/10.30574/ijsra.2026.19.1.0683

Abstract

The sustainable production of nano-cellulose acetate (CA) derived from waste cotton linter via a unique, simple route using a catalyst is the primary objective of this study. The cellulose was recovered from waste cotton linters through a sequence of chemical and mechanical treatments, including scouring, alkaline treatment, bleaching, washing, and drying conditions. The purified cellulose was then acetylated using varying amounts of acetic anhydride (AA) with time in the presence of acetic acid and sulfuric acid as a catalyst to evaluate the influence of reagent like sample 1 (32 mL AA+ Reaction Time (RT) 30 min), sample 2 (64 mL AA+RT 30 min), sample 3 (64 mL AA+ RT 60 min), sample 4 (96 mL AA+ RT 30 min). The characterization of the resulting nano CA was performed using Fourier transform infrared spectroscopy (FTIR), which confirmed the presence of the ester group characteristic of successful acetylation. Surface features and structural morphology were analyzed through scanning electron microscopy (SEM), revealing non-uniform particle distributions. The X-ray diffraction (XRD) analysis yields good results, with a crystallite size ranging from 3.0 to 6.0 nm. From the XRD data analyzed using the Scherrer equation, the crystallite sizes of nano CA for the four (4.0) samples were 6.09 nm, 3.93 nm, 3.81 nm, and 6.10 nm, respectively. This study reveals that discarded cotton linter can serve as a viable raw material for CA production, offering an eco-friendly and cost-effective alternative for polymer synthesis in chemical engineering.

Keywords: Cotton linter; Cellulose acetate; SEM; Waste to Wealth; XRD

1. Introduction

Organic fibers are eco-friendly and valuable for both the earth and humans [1]. The distinctive characteristics of organic fibers and the diverse applications have been used for the last few decades [2]. Due to environmental concerns and the high cost of synthetic fiber, natural fiber is replacing it. Natural fiber exhibits numerous benefits due to its biodegradability, cost-effectiveness, and environmental friendliness [3, 4]. The other concerns and applications of natural fiber include non-toxicity, renewable qualities, high specific strength, increased moisture absorption quality, outstanding thermal properties, and economic stability [5]. Cotton is recognized as a soft, tiny, slightly fibrous substance formed in the protective casing [6]. The cotton plant, which is found in bushes, is composed of approximately 94.0 % cellulose. Cotton is the natural fiber used for the production of nano-cellulose, and it possesses multiple attributes,

* Corresponding author: Md. Mazedul Haque Sachchu and Md. Shamsul Alam

including being easily obtainable, affordable, renewable, abundant, durable, enduring, and biodegradable [7]. Cotton swells in certain concentrated solutions, water, and excessively humid conditions [8, 9]. It is one of the purest natural sources of cellulose used in textiles and biomaterials since each cotton fiber is a long plant cell whose secondary wall is composed primarily of cellulose microfibers. The amount of cotton waste produced is staggering due to a steady rise in global cotton consumption [9]. A significant amount of this magnificent natural resource goes unused, as almost all of the cotton waste ends up in dumps or incinerators [10]. Cotton linters are short cellulose fibers that stay on the cotton seed coat after the longer spinnable fibers are removed during the ginning process [11, 12]. Cotton linters are typically unsuitable for textile applications due to their extremely low fiber length [12]. More than 75.0 % of the holo-cellulose in cotton linters is α-cellulose, making up over 80.0 % of the total. Cotton linters are a vital industrial raw material for the manufacturing of numerous cellulose-based goods, such as absorbent cotton, cellulose nitrate, and cellulose acetate, due to their high cellulose content and advantageous chemical makeup [13]. Additionally, cotton linters are a widely available source of high-purity cellulose for chemical and material applications since they are produced in enormous numbers as a byproduct of the cotton textile industry [14].

One of the most prominent polymers derived from plants is cellulose acetate, which is produced when the plant molecule cellulose is acetylated [13]. Textile fibers like acetate rayon, acetate-based yarn, or triacetate can be produced from cellulose acetate [15]. In addition, the chemical can be dissolved in particular solvents, melted or softened by heat, and then spun into fibers, molded into solid objects, or cast as films. The biodegradability of cellulose acetate is very high. As an ecologically sustainable material, cellulose acetate's chemical treatment influences its biodegradability in nature [16]. Cellulose acetate modified with acetic acid has an enhanced adsorption capacity compared to cellulose by itself. Cellulose acetate's improved absorbency enables it to absorb oils and organics in water because of its larger pore size, better hydrophobicity, and wettability [17]. Different studies concentrate on cellulose acetates as a value-added processing technique for high-purity cellulose feedstocks, which have numerous uses, particularly in filters, textiles, and films [18, 19]. Research on the degree to which feedstock parameters impact produced acetates is warranted in the field of cellulose acetate manufacture due to the strict requirements for feedstock quality [18]. Small levels of contaminants like lignin and leftover hemicelluloses can have a detrimental effect on high-quality acetate products, mainly optical films [19]. Cotton linters, byproducts of the cotton ginning process, have received interest for potential options [20]. This study will produce nano CA from waste cotton linter under different conditions and evaluate the samples for future utilization in different application fields.

2. Materials and Methods

2.1. Materials

Cotton linters were used as the primary raw material in this study. The cotton linters were collected from a local cotton-processing factory in Kushtia-7003, Bangladesh. In most cotton industries, cotton linters are considered a waste by-product generated during the processing of cotton fibers. However, these linters contain a high percentage of cellulose and therefore serve as an excellent raw material for the preparation of cellulose-based derivatives such as CA.

2.1.1. Chemicals and Reagents

All enlisted chemicals used in the experimental work were of analytical grade and were used without further purification. Sodium hydroxide (NaOH, 99.50 % purity) supplied by Merck, Germany, was used for the alkali treatment of cotton linters to remove impurities such as waxes, lignin, and hemicellulose. Sodium chlorite ($NaClO_2$, 98.0 % purity) obtained from BDH, England, was used as a bleaching agent to purify the cellulose fibers. Acetic acid (CH_3COOH, 99.80 % purity) supplied by Merck, Germany, served as the reaction medium during the acetylation process. Sulfuric acid (H_2SO_4, 98.0 % purity) from Merck, Germany, was used as a catalyst to facilitate the acetylation reaction. Acetic anhydride ($C_4H_6O_3$, 98.0 % purity), also supplied by Merck, Germany, was used as the acetylating agent for the synthesis of cellulose acetate.

2.2. Methods

2.2.1. Waste Cotton Linter Processing (Scouring)

The collected waste cotton linters were washed thoroughly with water to remove impurities such as dust and sand. The cleaned fibres were then dried in the sunlight [temperature 29 ºC, feel like 31 ºC] before further chemical treatment.

2.2.2. Alkali Treatment of Cotton Linter

About twenty (20.0) gm [ATY224, Shimazu, Japan] of cotton linters were dried in an electric oven at 105.0 °C [ED115, USA] until a constant weight was obtained. The dried fibres were then treated with 2.0 % (w/v) sodium hydroxide (NaOH) solution with a fibre-to-liquor ratio of 1:20 (w/w). The treatment was carried out at 80.0 °C [Thermo-Scientific, UK] for four (4.0) hours with occasional stirring to remove non-cellulosic materials such as lignin and hemicellulose. After treatment, the fibres were filtered, washed with distilled water and 2.0 % acetic acid solution until neutral pH was reached, then dried in an oven at 105.0 °C [ED115, USA] and stored in a desiccator.

2.2.3. Bleaching of Cotton Linter Cellulose

The alkali-treated fibres were bleached using 0.5 % sodium chlorite ($NaClO_2$) solution at 90.0 °C for 1.5 hours [Thermo-Scientific, UK] with a fibre-to-liquor ratio of 1:20 (w/w). The pH was maintained at about 4.0 [ORP, China] using an acetic acid and sodium acetate buffer solution. After bleaching, the fibres were washed thoroughly with distilled water and treated with 0.20 % sodium metabisulphite ($Na_2S_2O_5$) for 30.0 minutes. The fibres were then washed again and air-dried. The color of the fibres changed from brown to white, indicating purification of cellulose.

2.2.4. Preparation of nano Cellulose Acetate

Cellulose acetate was prepared through acetylation of purified cellulose. About four (4.0) gm of cellulose was mixed with 50.0 mL of glacial acetic acid and stirred for thirty (30.0) minutes. A solution of concentrated sulfuric acid in glacial acetic acid was then added as a catalyst. Acetic anhydride (AA) (32, 64, or 96.0 mL) was added to initiate the acetylation reaction.

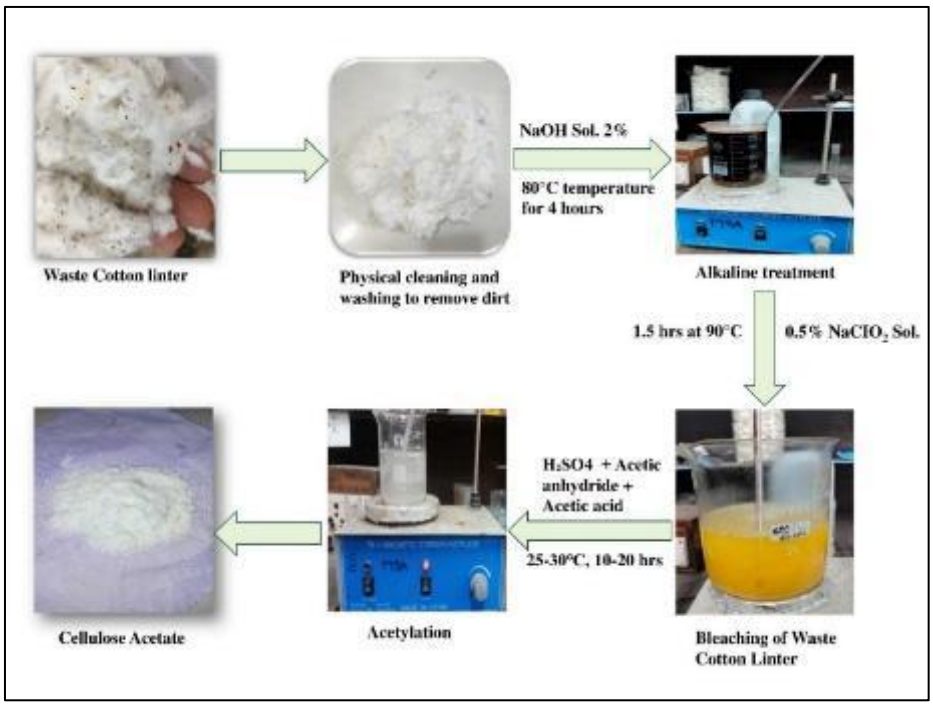

Figure 1 Preparation of nano CA from waste cotton linter

The mixture was stirred and allowed to react for several hours. Distilled water was then added to precipitate the product. The precipitated cellulose acetate was filtered, washed to neutral pH, and dried in an oven at 105.0 °C [ED115, USA]. We made four (4.0) nano samples by changing different conditions and parameters to evaluate the best performance and optimization. For example- Sample 1 (32.0 mL AA+ Reaction Time (RT) 30.0 min), Sample 2 (64.0 mL AA+RT 30.0 min), Sample 3 (64.0 mL AA+ RT 60.0 min), Sample 4 (96.0 mL AA+ RT 30.0 min).

3. Characterization

3.1. X-ray diffraction

The XRD analytical method was employed to investigate the crystal structure and crystal size of CA. The technique was used to determine the crystallite size [21, 22], phase identification [23, 24], lattice volume [25, 26], structure, d-spacing [27, 28], strain, and lattice parameters [29, 30], as well as axial parameters and angular parameters [31, 32]. The X-ray source was a Cu target operating at 40.0 kV × 50.0 mA (2.0 kW) [Smart Lab SE, Rigaku, Japan] [33, 34]. The instrument was configured in Bragg-Brentano (BB) geometry with CBO-BB optics. The primary X-ray beam passed through the Beryllium (Be) window and a 2.5° solar slit [35, 36]. The 1D scan mode was used to conduct the study, with a step size of 0.01° and a speed of 30.0°/minute [64, 65]. The length limiting slit is 10.0 mm, the incidence slit box is 1-2°, and the scan ranges (2θ) are 5.0 to 90.0° [37, 38]. The receiving slit boxes 1 and 2 of the theta-theta goniometer are open, and the investigation was performed using the Hypix-400 horizontal HPAD (1D) open detector [39, 40]. The crystallite size was determined from XRD measurements [66, 67] by using the Debye-Scherrer formula [41, 42].

$$D = \frac{k\lambda}{\beta \operatorname{Cos} \theta} \qquad (1)$$

Here, crystallite size is denoted as D, λ= wavelength of the X-ray source [Cu tube; λ= 0.1541 nm], K = crystallite-shape factor (0.9), β= full width at half maximum, and θ= diffraction angle [43].

3.2. Fourier Transform Infrared Spectroscopy

The synthesized nanoparticles were analyzed using Fourier transform infrared (FTIR) spectroscopy with the SHIMADZU IRAffinity-1S instrument in attenuated total reflectance (ATR) mode. Spectral data were collected at a resolution of 4.0 cm^{-1} over a broad wavenumber range of 400.0 to 4000.0 cm^{-1} to accurately identify molecular vibrations and associated functional groups within the sample.

3.3. Scanning Electron Microscopy

The morphology and elemental composition of the synthesized samples 1 to 4 were characterized using SEM and EDX analysis [44, 45]. The shape and surface features of the nanoparticles were examined with a ZEISS Sigma 500 VP field emission scanning electron microscope (FESEM), operated at 5 kV, with magnifications of 20,000 and 50,000 times.

4. Result and Discussion

4.1. X-ray Crystallographic Phase Analysis

By X-ray diffractogram analysis, the crystalline size of nano CA samples 1 to 4 was calculated. The following XRD is shown for the four (4.0) samples. All the samples favor the formation of nano CA. For sample 1, the synthesized compound exhibited distinct diffraction peaks at 2θ values of 15.00°, 16.69°, 20.41°, 22.62°, and 25.70° corresponding to crystallite sizes of 4.0, 6.3, 13.8, 4.0, and 2.3 nm, respectively. For sample 2, the synthesized compound exhibited distinct diffraction peaks at 2θ values of 23.14°, 26.4°, 27.45°, 35.22°, and 47.36° corresponding to crystallite sizes of 4.27, 2.2, 2.9, 7.5, and 2.8 nm, respectively.

For sample 3, the synthesized compound exhibited distinct diffraction peaks at 2θ values of 14.86°, 16.88°, 22.91°, 26.00°, and 28.76° corresponding to crystallite sizes of 7.2, 2.8, 4.29, 2.9, and 1.87 nm, respectively. For sample 4, the synthesized compound exhibited distinct diffraction peaks at 2θ values of 15.36°, 20.96°, 23.24°, 34.99°, and 42.41° corresponding to crystallite sizes of 2.84, 5.1, 4.6, 5.1, and 12.8 nm, respectively.

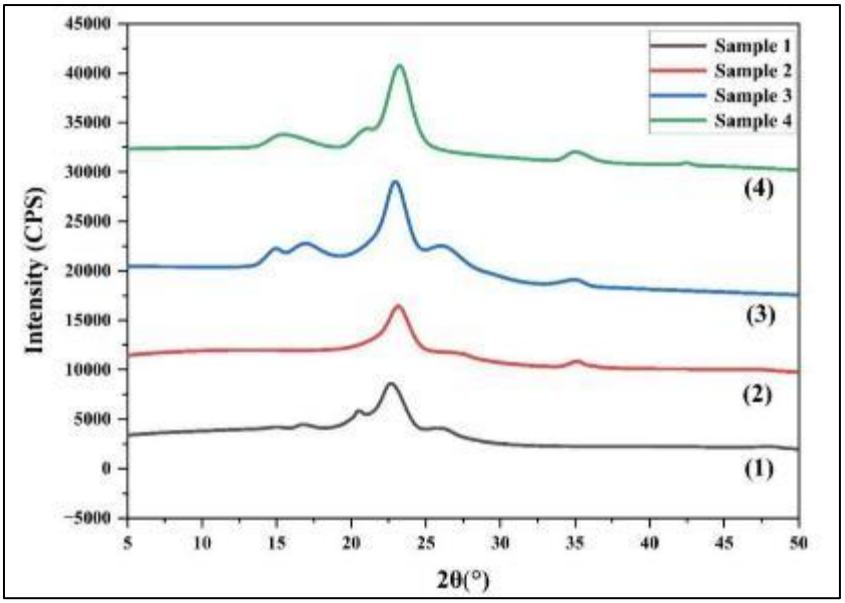

Figure 2 X-ray diffractogram of sample 1, sample 2, sample 3, and sample 4

Table 1 Grain size calculation of crystalline CA.

Sample	2 Theta (2θ)	(θ)	FWHM (radians)	Intensity, I (CPS°)	Crystallite size (D) (nm)	d-spacing (nm)
Sample 1	15.00	7.50	0.036652	885	4.00	0.5900
	16.69	8.34	0.023213	560	6.30	0.5310
	20.41	23.94	0.010647	542	13.80	0.4348
	22.62	10.20	0.036303	11,375	4.06	0.3928
	25.70	12.85	0.066323	2683	2.30	0.3500
Sample 2	23.14	11.57	0.034558	11,028	4.27	0.3841
	26.40	13.20	0.068068	947	2.20	0.3380
	27.45	13.72	0.052360	1008	2.90	0.3247
	32.22	16.11	0.020246	768	7.50	0.2546
	47.36	23.68	0.055851	806	2.80	0.1918
Sample 3	14.86	7.43	0.020420	1078	7.20	0.5960
	16.88	8.44	0.052360	7145	2.80	0.5250
	22.91	11.45	0.034383	18,763	4.29	0.3879
	26.00	13.00	0.052360	6115	2.90	0.3424
	28.76	14.38	0.080285	2569	1.87	0.3101
Sample 4	15.36	7.68	0.051487	2899	2.84	0.5765
	20.96	10.48	0.029147	2622	5.10	0.4236
	23.24	11.62	0.031590	12,256	4.69	0.3824
	34.99	17.49	0.029845	1298	5.10	0.2562
	42.41	21.20	0.012217	162	12.80	0.2129

Specifically, the observed diffraction peaks and corresponding interplanar spacing (d-values in nm) in Table 1 were as follows: for sample 1, 15.00 (0.59 nm), 16.69 (0.531 nm), 20.41 (0.4348 nm), 22.62 (0.3928 nm), and 25.70 (0.35 nm). For sample 2, 23.14 (0.3841 nm), 26.40 (0.338 nm), 27.45 (0.3247 nm), 32.22 (0.2546 nm), and 47.36 (0.1918 nm). For sample 3, 14.86 (0.596 nm), 16.88 (0.525 nm), 22.91 (0.3879 nm), 26.00 (0.3424 nm), and 28.76 (0.3101 nm). For sample 4, 15.36 (0.5765 nm), 20.96 (0.4236 nm), 23.24 (0.3824 nm), 34.99 (0.2562 nm), and 42.41 (0.2129 nm).

The synthesized compounds of different samples exhibited prominent diffraction peaks corresponding to the three most intense Bragg reflections, as shown in Fig. 3.

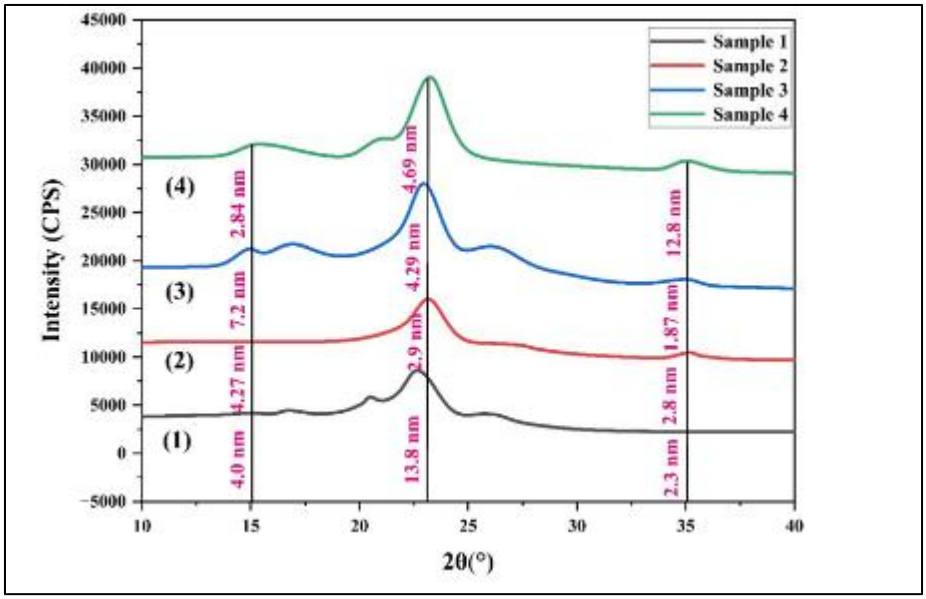

Figure 3 XRD illustration of sample 1, sample 2, sample 3, and sample 4.

The uniformity of orientation within the crystal lattice was further examined using peak profiling analysis [46, 47]. According to Table 2, the peak profiling values for samples 1, 2, 3, and 4 were (17, 31, 49), (40, 56, 161), (16, 39, 61), and (17, 40, 130), respectively, based on the three most intense Bragg positions.

Table 2 Peak profiling by diffraction Bragg's angle.

Sample	Diffraction angle (2θ)	θ	1000×Sin²θ	Crystallite size (D) (nm)
Sample 1	15.00	7.50	17	4.0
	20.41	10.205	31	13.80
	25.70	12.85	49	2.30
Sample 2	23.14	11.57	40	4.27
	27.45	13.725	56	2.90
	47.36	23.68	161	2.80
Sample 3	14.86	7.43	16	7.20
	22.91	11.455	39	4.29
	28.76	14.38	61	1.87
Sample 4	15.36	7.68	17	2.84
	23.24	11.62	40	4.69
	42.41	21.205	130	12.80

4.1.1. Average size calculation

The crystallite size of the prepared samples is determined by the Debye-Scherrer equation [48, 49], calculated based on equation 1 [50, 51].

Table 3 The average crystallite size calculation of the synthesized samples 1 to 4.

Sample Name	Crystallite size (nm)
Sample 1	6.09
Sample 2	3.93
Sample 3	3.81
Sample 4	6.10

The crystallite size determined by the Scherrer equation of these samples is 6.09 nm, 3.93 nm, 3.81 nm, and 6.10 nm, respectively. The smallest crystal size is obtained for sample 3 (64 ml AA, RT 60 min).

4.2. Fourier Transform Infra-Red Analysis

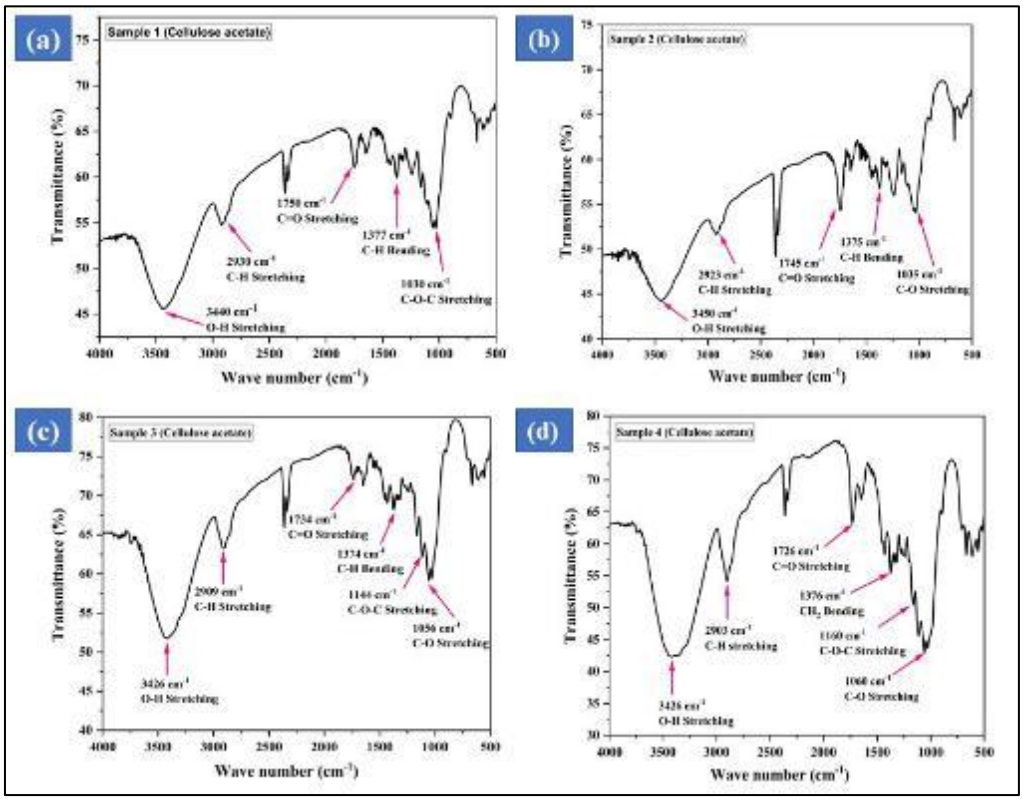

Figure 4 FTIR spectra of CA samples (a) sample 1, (b) sample 2, (c) sample 3, and (d) sample 4

FTIR is used to analyze the specific functional group. In this investigation, four (4.0) samples were evaluated, and the ester group was obtained, proving the functionality and acetylation. All samples' FTIR spectra (Fig. 4 a-d) show the distinctive vibrational fingerprints of CA, indicating successful cellulose backbone acetylation. The existence of residual hydroxyl groups and incomplete substitution is indicated by a broad absorption band at 3426 to 3450 cm^{-1}, which is attributable to O–H stretching. Samples 3 and 4 show a modest red shift that suggests stronger intermolecular hydrogen bonding. The aliphatic C–H stretching of acetyl methyl groups is represented by the bands at 2903 to 2930 cm^{-1}. Additionally, wavenumbers 1734 and 2903 cm-1, which corresponded to C=O and CH vibrations, respectively, showed an increase in intensity [52].

The degree of acetylation substitution is shown by the peak height ratio of the carbonyl functional group to the adsorbed water band (1735/1651) [53]. Ester carbonyl (C=O) stretching is responsible for a prominent absorption peak in the

range of 1726 to 1750 cm^{-1}, which provides conclusive proof of acetylation; its systematic shift toward lower wavenumbers from sample 1 to sample 4 reflects changes in the local chemical environment, probably related to variations in the degree of substitution and polymer chain interactions. Methyl groups' C–H bending vibrations are responsible for the bands at 1374 to 1377 cm^{-1}, whilst the glycosidic and ester linkages' C–O and C–O–C stretching vibrations are responsible for the area between 1030 and 1160 cm^{-1}. Samples 3 and 4 have higher spectral complexity and intensity in this area, which point to improved substitution and structural reorganization. Collectively, these results confirm the formation of cellulose acetate with discernible variations in substitution level and molecular organization across the samples.

4.3. Scanning Electron Microscopy and Energy Dispersive X-ray Spectroscopy Analysis

SEM analysis of the four cellulose acetate samples is described below, with some analytical points. The surface morphology of cellulose acetate synthesized from cotton linter was examined through SEM. Multiple images of the same sample were taken at varying magnifications and viewing angles to better understand the material's microstructural features. The successful production of cellulose acetate is demonstrated by the SEM examination in Fig. 5. At 500X magnification, Fig. 5 (a) and (c) show a consistent distribution of these elongated structures, suggesting a robust and repeatable synthesis process. The surface topography is better seen in the high-magnification micrograph in Fig. 5 (b) at 2000 magnification. It appears to be relatively smooth with faint longitudinal striations, indicating a distinct outer wall or sheath. On the other hand, Fig. 5 (d) shows an architecture that is more entwined and web-like, which is indicative of higher polymer chain entanglement. Because it increases the effective surface area accessible for molecular interaction, this interconnected network is very suitable for applications in scaffolding or water treatment [54, 55, 56].

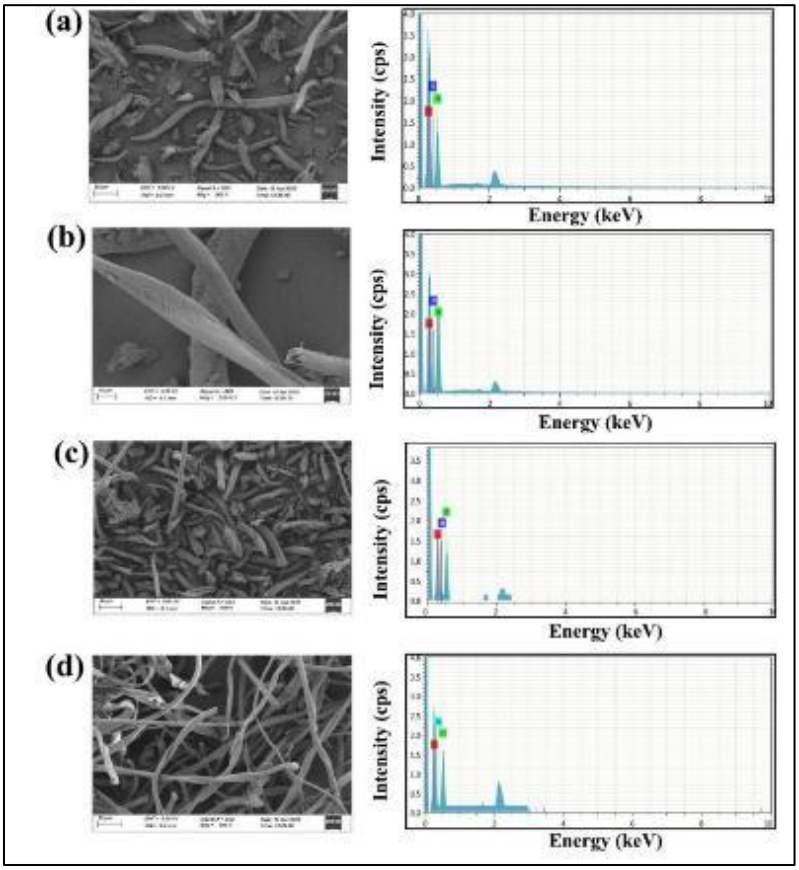

Figure 5 Surface morphology and EDX spectra of (a) sample 1, (b) sample 2, (c) sample 3, and (d) sample 4

The EDX spectroscopy was used to assess the elemental profile and chemical purity of the produced microstructures; the resulting spectra for samples 1 to 4 are shown in Fig. 5. Carbon (C ≈ 0.277 keV), nitrogen (N ≈ 0.392 keV), and oxygen (O ≈ 0.525 keV) all showed strong and consistent elemental signatures. The Gold (Au) Mα line, which was inserted during the sputter-coating process to reduce charging effects on the non-conductive organic surface, is probably responsible for the persistent occurrence of a tiny peak at about 2.1 keV. The O/C and N/C relative intensity ratios for each of the samples 1 to 4 show a high level of chemical uniformity.

5. Possible Applications

By analyzing different investigations like XRD, SEM, and EDX, we can utilize the obtained CA in different functional applications. Below is a table for different studies on CA.

Table 4 Functional applications of the CA.

Serial No.	Functional Application	References
1	Cigarette filters, mainly made from CA fibers, create serious environmental problems because they degrade very slowly and may release toxic substances. This study was conducted to thoroughly examine and compare the physicochemical and thermomechanical properties of CA fibers taken from both unused and used cigarette filters.	[57]
2	Acetate has long been widely used in various textile applications due to its favorable properties and excellent processing performance. It is utilized in woven, knitted, and braided fabrics, and appears in a wide range of products such as medical gauze, ribbons, coffin linings, home furnishings, velvet fabrics, tricot and circular knits, men's and women's linings, satins, and other fashion textiles.	[58, 59]
3	CA and its modified polymer-based materials have long been utilized for removing heavy metals from wastewater. CA is an eco-friendly polysaccharide that is widely available and exhibits strong hydrophilicity along with excellent film-forming properties. These characteristics make it highly suitable for use in various membrane technologies, including ultrafiltration, nanofiltration, reverse osmosis, and forward osmosis.	[60]
4	New coatings for the polarographic oxygen electrode based on CA derivatives are presented. Compared to traditional collodion coatings, these materials offer several benefits, including the formation of highly durable membranes and improved stability of the electrode.	[61]
5	Electrospinning has emerged as a novel approach to explore the exceptional material properties of cellulose acetate (CA). Electrospun CA nanofibers have been widely used in therapeutic applications, incorporating antimicrobial substances, antibacterial nanoparticles, antioxidants, as well as systemic and anti-inflammatory agents.	[62]
6	Cellulose derivatives are mainly classified into two groups: cellulose ethers and cellulose esters, each having distinct physicochemical and mechanical properties. These polymers are widely utilized in the development of pharmaceutical dosage forms and healthcare products. They play significant roles in various applications, including extended and delayed-release coatings, controlled-release matrices, osmotic drug delivery systems, bioadhesive and mucoadhesive formulations, and as compressibility enhancers in tablets. Additionally, they function as thickening agents and stabilizers in liquid formulations, binders in granules and tablets, and gelling agents in semisolid preparations, along with many other uses.	[63]

Figure 6 Functional applications of CA.

6. Conclusion

The experimental analysis showed that the amount of AA and the RT significantly influence the degree of cellulose acetylation. Elemental analysis using EDX spectroscopy confirmed that successful acetylation is indicated by an increase in oxygen content and a decrease in carbon content, demonstrating that acetyl groups have substituted hydroxyl groups within the cellulose structure. Of the four samples examined, sample 3 had the highest oxygen content (47.48 %) and a relatively low carbon content (42.76 %), indicating optimal conditions for efficient acetylation. Conversely, sample 1 exhibited a higher carbon content and lower oxygen percentage, reflecting a substantially lower degree of substitution. The results clearly suggest that increasing hydrolysis time results in more nano CA molecules undergoing hydrolysis, thereby increasing the hydrolysis rate. This is due to the prolonged exposure of cellulose acetate to hydrolysis agents, which allows more ester bonds to break down, an effect confirmed by the FTIR analysis. The SEM analysis revealed an increase in the accessible surface area for molecular interaction, forming an interconnected network suitable for applications in scaffolding or water treatment. The XRD analysis showed that the crystallite sizes were 6.09 nm, 3.93 nm, 3.81 nm, and 6.10 nm for the respective samples 1 to 4 for the nano conformation, where sample 3 had the smallest crystallite size. Monitoring elemental changes related to acetylation efficiency was facilitated by EDX, providing a solid basis for improving production procedures and ensuring uniform quality of nano CA for future applications.

Compliance with ethical standards

Acknowledgments

The author's heartiest thanks to Dr. Sharif Md. Al-Reza, Chairman, Department of Applied Chemistry and Chemical Engineering (ACCE), Islamic University, Kushtia-7003, Bangladesh, for cooperation in this research and for providing laboratory facilities. We also expressed thanks to Dr. Shirin Akter Jahan, PSO, IGCRT, BCSIR, Bangladesh, for using the PC, software, and other appliances.

Disclosure of conflict of interest

The authors declared that there are no known conflicts or financial interests that could influence this manuscript.

Data Availability

Data will be available on request.

Credit Author Contributions Statements

Nusrat Zahan: Experiment, original draft, Visualisation, Validation, Resources, Methodology, Data curation. Md. Mazedul Haque Sachchu: Writing-original draft, Visualisation, Validation, Resources, Methodology, Discussion, Investigation, Formal analysis, Data curation, Software. Mohshin Maola: Writing-original draft, Visualisation, Validation, Resources, Discussion, Investigation, Formal analysis, Data curation. Md. Tauhidul Islam: Writing-original draft, Investigation, Formal analysis, Data curation. Md. Ralin Islam: Writing-original draft, Investigation, Formal analysis, Data curation. Anik Biswas: Writing-original draft, Investigation, Formal analysis, Data curation. Tumpa Rani Kar: Formal analysis, Data curation. Md. Ashraful Alam: Writing-review & editing, technical advice, Resources, Data curation, Investigation, Formal analysis, Software. Md. Shamsul Alam: Writing-review & editing, technical advice, Software, Resources, Methodology, Data curation, Conceptualization, Supervision.

References

[1] Jaiswal D, Devnani GL, Rajeshkumar G, Sanjay MR, Siengchin S. Review on extraction, characterization, surface treatment and thermal degradation analysis of new cellulosic fibers as sustainable reinforcement in polymer composites. Current Research in Green and Sustainable Chemistry. 2022 Jan 1;5:100271.

[2] Kicińska-Jakubowska A, Bogacz E, Zimniewska M. Review of natural fibers. Part I—Vegetable fibers. Journal of Natural Fibers. 2012 Jul 1;9(3):150-67.

[3] Omrani E, Menezes PL, Rohatgi PK. State of the art on tribological behavior of polymer matrix composites reinforced with natural fibers in the green materials world. Engineering Science and Technology, an International Journal. 2016 Jun 1;19(2):717-36.

[4] Singh AS, Halder S, Kumar A, Chen P. Tannic acid functionalization of bamboo micron fibes: Its capability to toughen epoxy based biocomposites. Materials Chemistry and Physics. 2020 Mar 1;243:122112.

[5] Dayan AR, Habib M, Kaysar MA, Uddin M. Study on the physico-mechanical properties of okra fibre at different harvesting time. Saudi J. Eng. Technol. 2020;5:304-9.

[6] Kumar P, Sai Ram C, Srivastava JP, Behura AK, Kumar A. Synthesis of cotton fiber and its structure. Natural and Synthetic Fiber Reinforced Composites: Synthesis, Properties and Applications. 2022 Feb 14:17-36.

[7] Rizal S, HPS AK, Oyekanmi AA, Gideon ON, Abdullah CK, Yahya EB, Alfatah T, Sabaruddin FA, Rahman AA. Cotton wastes functionalized biomaterials from micro to nano: a cleaner approach for a sustainable environmental application. Polymers. 2021 Mar 24;13(7):1006.

[8] Theivasanthi T, Christma FA, Toyin AJ, Gopinath SC, Ravichandran R. Synthesis and characterization of cotton fiber-based nanocellulose. International journal of biological macromolecules. 2018 Apr 1;109:832-6.

[9] Ruiz-Caldas MX, Carlsson J, Sadiktsis I, Jaworski A, Nilsson U, Mathew AP. Cellulose nanocrystals from postconsumer cotton and blended fabrics: a study on their properties, chemical composition, and process efficiency. ACS Sustainable Chemistry & Engineering. 2022 Mar 2;10(11):3787-98.

[10] Liang D, Liu W, Zhong T, Liu H, Dhandapani R, Li H, Wang J, Wolcott M. Nanocellulose reinforced lightweight composites produced from cotton waste via integrated nanofibrillation and compounding. Scientific Reports. 2023 Feb 7;13(1):2144.

[11] Negm M, Sanad S. Cotton fibres, picking, ginning, spinning and weaving. InHandbook of Natural Fibres 2020 Jan 1 (pp. 3-48). Woodhead Publishing.

[12] Sczostak A. Cotton linters: an alternative cellulosic raw material. InMacromolecular Symposia 2009 Jun (Vol. 280, No. 1, pp. 45-53). Weinheim: WILEY-VCH Verlag.

[13] Shaheen W, Iqbal MM, Qudrat L. Development of cellulose-based superabsorbent polymers: a review. Cellulose. 2025 Mar;32(5):2811-45.

[14] Morais JP, de Freitas Rosa M, Nascimento LD, Do Nascimento DM, Cassales AR. Extraction and characterization of nanocellulose structures from raw cotton linter. Carbohydrate polymers. 2013 Jan 2;91(1):229-35.

[15] Zolriasatein AA. Effect of lipase treatment on physical and dyeing properties of cellulose acetate fabric. Recent Innovations in Chemical Engineering (Formerly Recent Patents on Chemical Engineering). 2020 Nov 1;13(5):344-52.

[16] Ganster J, Fink HP. Cellulose and cellulose acetate. Bio-Based Plastics: Materials and Applications. 2013 Nov 13:35-62.

[17] Fauzi FA, Mohamad F. Utilising Cellulose Acetate Derived from Cotton Waste for Efficient Oil Removal in Water. Future Energy and Environment Letters. 2024 Dec 26;1(1):1-8.

[18] Olaiya NG, Al-Amin M, Rashed K, Maraveas C. Nanomaterials from Textile Waste for Purification and Environmental Applications. Polymers. 2025 Nov 21;17(23):3098.

[19] Anik FK, Alam MA, Bishwas RK, Sachchu MM, Mohsin M, Jahan SA. Effect of Hydrolysis Catalyst and Photo-catalysis Performance Exploration of Rutile Nanocrystal Derived from Screen Printing Waste: A Waste to Wealth Approach. Chemistry of Inorganic Materials. 2025 Nov 21:100131.

[20] Mullins EP. Utilization of cotton ginning byproduct and whole cottonseed as a feed source in growing cattle. North Carolina State University; 2021.

[21] Sachchu MM, Anik FK, Ahmed S, Aman S, Podder U, Sayeem NR, Islam MT, Rahaman MA, Hossain J, Khatun MM, Alam MA. Crystallographic investigation of PVA@ PLA nanocomposite film by X-ray diffraction: insight from high resolution TEM. Journal of Engineering Research and Reports. 2025 Mar 7;27(3):310-27.

[22] Hossain J, Sachchu MM, Ahmed S, Sadia SI, Shishir MK, Sayeem NR, Podder U, Israt A, Rahman A, Haque NN, Anik FK. Reinforcement of Biodegradable PLA-PVA Composite Films with Carbon Nanotubes: Mechanical and Thermal Property Analysis. Journal of Materials Science Research and Reviews. 2025 Feb 2;8(1):110-23.

[23] Tabassum S, Hossain MS, Sachchu MM, Uddin MN, Ahmed S. Green synthesis of nano-Ag 2 O using Moringa oleifera leaves for efficient photocatalytic and antimicrobial applications. New Journal of Chemistry. 2025;49(4):1301-13.

[24] Sachchu MM, Hasan M, Hossain MK, Ahmed S, Eva TN, Lima MN, Hossain A, Alam MA. Heavy metal contamination in Pangas Catfish of farm ponds aquaculture in different locations in Bangladesh: A risk assessment study. Food Chemistry Advances. 2025 Sep 1;8:101044.

[25] Sachchu MM, Tama RT, Hossain MS, Hoque NS, Hossain MK, Lima NJ, Hasan M, Bishwas RK, Haque NN, Alam MA. Physicochemical and Microbiological Assessment of Low Rainfall and Extreme Weather Conditions: A Case Study on Tropic of Cancer in Bangladesh. Asian Journal of Research in Biochemistry. 2025 Apr 8;15(2):174-93.

[26] Sachchu MM, Hossain A, Kobir MM, Hoda MD, Ahamed MR, Lima MN, Eva TN, Alam MA. Heavy metal intake by fishes of different river locations in Bangladesh: A comparative statistical review. Asian Journal of Fisheries and Aquatic Research. 2024 Jun 11;26(6):43-67.

[27] Al-Mahmud MR, Shishir MK, Ahmed S, Tabassum S, Sadia SI, Sachchu MM, Tama RT, Miah AR, Alam MA. Stoichiometry crystallographic phase analysis and crystallinity integration of silver nanoparticles: A Rietveld refinement study. Journal of Crystal Growth. 2024 Oct 1;643:127815.

[28] Ahmed S, Shishir MK, Sadia SI, Al-Reza SM, Sachchu MM, Aidid AR, Islam MM, Al-Mahmud MR, Rana MM, Alam MA. Crystallographic phase biographs of copper nanocrystalline material: A statistical perspective review. Nano-Structures & Nano-Objects. 2024 Sep 1;39:101275.

[29] Shishir MK, Afrin S, Sachchu MM, Eva TN, Tabassum S, Ahmed S, Sadia SI, Alam MA. Crystalline copper nanomaterials for advanced ceramic: a comprehensive review for functional ceramic coating approaches. Asian Journal of Advanced Research and Reports. 2024 Jul 4;18(8):13-34.

[30] Alam MA, Bishwas RK, Mostofa S, Jahan SA. Impact on preferred orientation and crystal strain behavior of nanocrystal anatase-TiO2 by X-ray diffraction technique. South African Journal of Chemical Engineering. 2024 Jul 1;49:348-52.

[31] Alam MA, Tabassum M, Mostofa S, Bishwas RK, Sarkar D, Jahan SA. The effect of precursor concentration on the crystallinity synchronization of synthesized copper nanoparticles. Journal of Crystal Growth. 2023 Nov 1;621:127386.

[32] Alam MA, Ahmed S, Bishwas RK, Mostofa S, Jahan SA. X-ray crystallographic diffraction study by whole powder pattern fitting (WPPF) method: Refinement of crystalline nanostructure polymorphs TiO2. South African Journal of Chemical Engineering. 2025 Jan 1;51:68-77.

[33] Sayeem NR, Podder U, Alam MA, Shishir MK, Miah MA, Anik FK, Ghosh P, Ahmed S, Islam M, Jahan SA. Critical perspective review on green synthesis of zinc oxide nanoparticles: Explored wurtzite phase, characterization and real world applications. Next Nanotechnology. 2026 Jun 1;9:100412.

[34] Alam MA, Bishwas RK, Zannat F, Jahan SA. Crystallographic Exploration of Copper Nanocrystal by X-ray and Selected Area Electron Diffraction Pattern: High Resolution Transmission Electron Microscopy Insight. Physics Letters A. 2026 Jan 20:131391.

[35] Alam MA, Bishwas RK, Mostofa S, Ahmed S, Zannat F, Jahan SA. Study of Sol-Gel Derived Silver Nanoparticle (AgNPs): X-ray Computed Crystal Growth Mechanism and Thermal Analysis. South African Journal of Chemical Engineering. 2026 Jan 28:100839.

[36] Hossain A, Sachchu MM, Shishir MK, Sayeem NR, Podder U, Al-Mahmud MR, Al Rashid MM, Tama RT, Haque NN, Rahman A, Alam MA. Profile of Lipid and Antioxidant Activity Lipids Extracted from Pangasius pangasius: Complementary Analysis. ASIAN JOURNAL OF RESEARCH IN BIOCHEMISTRY Учредители: Sciencedomain International. 2024 Dec 23;14(6):199-212.

[37] Alam MA, Bishwas RK, Ahashan SM, Miah MA, Rahaman MA, Islam MT, Zannat F, Al Mamun MZ, Jahan SA. Crystallography Phase Analysis of Copper Oxide Nanocrystal by X-ray Diffraction and Selected Area Electron Diffraction: A Comprehensive Exploration. Materials Today Communications. 2026 Mar 24:115057.

[38] Das G, Hossain Shishir MK, Bayzid T, Mustak MH, Alam MA, Uddin MH, Khan GM. Valorization of Silk Waste Sericin Through Zinc Oxide Nanoparticles Biosynthesis for Toxic Dye Degradation. ChemistrySelect. 2026 Mar;11(9):e04728.

[39] Alam MA, Shishir MK, Podder U, Hasan MR, Rahaman MA, Islam MT, Rahman A. Crystallographic bibliography of Co-precipitate derived (311) Guite (Co3O4) crystalline materials. Next Nanotechnology. 2026 Jun 1;9:100392.

[40] Zannat F, Alam MA, Bishwas RK, Jahan SA. Crystallographic integration of highly preferred orientated peptization derived nano anatase TiO2. Journal of Crystal Growth. 2025 Dec 15:128462.

[41] Rahaman MM, Saha S, Shaha CK, Alam MA, Akhtar US, Karmaker S, Saha TK. A Comprehensive Study on the Adsorption of Ciprofloxacin Using Chitosan: Spectroscopic, DFT, Kinetic, Isotherm, Thermodynamic, and Reusability Insights. Desalination and Water Treatment. 2026 Jan 6:101631.

[42] Shishir MK, Alam MA, Bishwas RK, Karim MM, Alam SN, Khan GM. Crystallographic insights into copper oxide nanoparticles synthesized via a unique sol-gel method: antibacterial activity and photocatalytic evaluation. South African Journal of Chemical Engineering. 2025 Nov 10.

[43] Mohshin JN, Ahmed ST, Aidid AR, Sayeem NR, Yasmin H, Alam MA, Khanam J, Ganguli S, Chakraborty AK. Powder X-ray peak diffraction pattern of iron (II) tungstate (FeWO4): Crystallite size and strain analysis, and adsorption of methylene blue. Nano-Structures & Nano-Objects. 2025 Dec 1;44:101574.

[44] Shishir MK, Islam M, Sayeem NR, Anam NS, Shipon MR, Rifat M, Ahmed S, Tauhiduzzaman M, Alam MA. Comprehensive synthesis route of crystalline copper oxide nanoparticles: a crystallographic analysis with functional application. Chemistry of Inorganic Materials. 2025 Oct 17:100123.

[45] Ghosh P, Bishwas RK, Alam MA, Zannat F, Mohsin M, Jahan SA. Effect of Reaction Medium on Crystallinity and Morphological Properties of Precipitation-Derived α-Alumina Nanocrystals. Chemistry of Inorganic Materials. 2025 Oct 9:100124.

[46] Kawsar M, Hossain MS, Bahadur NM, Ahmed S. Synthesis of nano-crystallite hydroxyapatites in different media and a comparative study for estimation of crystallite size using Scherrer method, Halder-Wagner method size-strain plot, and Williamson-Hall model. Heliyon. 2024 Feb 15;10(3).

[47] Hossain MS, Ahmed S. Sustainable synthesis of nano CuO from electronic waste (E-waste) cable: evaluation of crystallite size via Scherrer equation, Williamson-Hall plot, Halder-Wagner model, Monshi-Scherrer model, size-strain plot. Results in Engineering. 2023 Dec 1;20:101630.

[48] Shishir MK, Alam MA, Rahaman MA, Islam MT, Rahman A, Hasan MR, Hasan M, Jahan SA. Crystallinity integration of Co-precipitate derived cubic bunsenite (NiO) phase crystalline nanomaterials. Results in Materials. 2025 Sep 30:100763.

[49] Alam MA, Ahmed S, Sarkar D, Bishwas RK, Jahan SA. Preferred crystallographic design of monoclinic tenorite (CuO) nanocrystals by powder X-ray line diffraction. Chemistry of Inorganic Materials. 2025 Sep 19:100119.

[50] Bishwas RK, Alam MA, Jahan SA. Crystallographic and morphological characterization of high-crystalline α-alumina nanoparticles: A comprehensive X-ray diffraction and transmission electron microscopy study. Chemical Physics Letters. 2025 Nov 1;878:142245.

[51] Zannat F, Alam MA, Ghosh P, Bishwas RK, Jahan SA. Sustainable synthesis of α-alumina nanoparticles: a comparative study of base-mediated crystallization via co-precipitation. Materials Advances. 2025;6(22):8431-47.

[52] Harvey AC, Adebayo AS, Wheatley AO, Asemota HN, Riley CK. Effects of acetylation on the micromeritics of yam (Dioscorea sp.) starch powder for pharmaceutical application. West African Journal of Pharmacy. 2012 Nov 1;23(2):40-50.

[53] Maryana R, Anwar M, Suwanto A, Hasanah SU, Fitriana E. Comparison study of various cellulose acetylation methods from its IR spectra and morphological pattern of cellulose acetate as a biomass valori. Nature Environment and Pollution Technology. 2020 Jun 1;19(2):669-75.

[54] Tiller P, Park S, Sanders J, Treasure T, Park S. Evaluating the quality and processability of cotton linter-derived cellulose acetate by characterization of native and artificial fines. Cellulose. 2025 Mar;32(5):2989-3005.

[55] Islam MD, Uddin FJ, Rashid TU, Shahruzzaman M. Cellulose acetate-based membrane for wastewater treatment—A state-of-the-art review. Materials Advances. 2023;4(18):4054-102.

[56] An Y, Li F, Di Y, Zhang X, Lu J, Wang L, Yan Z, Wang W, Liu M, Fei P. Hydrophobic modification of cellulose acetate and its application in the field of water treatment: a review. Molecules. 2024 Oct 30;29(21):5127.

[57] Wilkinson E, Hoh E, Stack M, Mladenov N, Youssef G. Thermal, physical, chemical, and mechanical properties of cellulose acetate from cigarette filters. Journal of Applied Polymer Science. 2025 Jun 10;142(22):e56946.

[58] Law RC. 5. Applications of cellulose acetate 5.1 Cellulose acetate in textile application. InMacromolecular symposia 2004 Mar (Vol. 208, No. 1, pp. 255-266). Weinheim: WILEY-VCH Verlag.

[59] Puls, Juergen, Steven A. Wilson, and Dirk Hölter. "Degradation of cellulose acetate-based materials: a review." Journal of Polymers and the Environment 19, no. 1 (2011): 152-165.

[60] Islam MD, Uddin FJ, Rashid TU, Shahruzzaman M. Cellulose acetate-based membrane for wastewater treatment—A state-of-the-art review. Materials Advances. 2023;4(18):4054-102.

[61] Hagihara B, Ishibashi F, Sasaki K, Kamigawara Y. Cellulose acetate coatings for the polarographic oxygen electrode. Analytical Biochemistry. 1978 Jun 1;86(2):417-31.

[62] Khoshnevisan K, Maleki H, Samadian H, Shahsavari S, Sarrafzadeh MH, Larijani B, Dorkoosh FA, Haghpanah V, Khorramizadeh MR. Cellulose acetate electrospun nanofibers for drug delivery systems: Applications and recent advances. Carbohydrate polymers. 2018 Oct 15;198:131-41.

[63] Shokri J, Adibkia K. Application of cellulose and cellulose derivatives in pharmaceutical industries. InCellulose-medical, pharmaceutical and electronic applications 2013 Aug 29. IntechOpen.

[64] Akhtar, Umme Sarmeen, Mohammad Golam Mostafa, Md Sagirul Islam, Md Ashraful Alam, Imdadul Haque, Shirin Akter Jahan, Gorungo Ray, Tanvir Ahmed, Debasish Sarkar, and Md Aftab Ali Shaikh. "Kaolinite based admixture for rapid hardening high strength concrete." Discover Civil Engineering 3, no. 1 (2026): 73.

[65] Ghosh, Pulak, Raton Kumar Bishwas, Md Ashraful Alam, Mohammad Mohsin, Md Saiful Quddus, and Shirin Akter Jahan. "Waste-Derived Surface-Active Nanostructured γ-Al2O3 for Efficient Dye Adsorption." Sustainable Chemistry One World (2026): 100210.

[66] Alam, Md Ashraful, Salma Akter Munni, Sabrina Mostafa, Raton Kumar Bishwas, and Shirin Akter Jahan. "An investigation on synthesis of silver nanoparticles." Asian Journal of Research in Biochemistry 12, no. 3 (2023): 1-10.

[67] Alam, Md Ashraful, Mobashsara Tabassum Mobashsara, Sabrina Mostofa Sabrina, Raton Kumar Bishwas Bishwas, Debasish Sarkar Debasish, and Shirin Akter Jahan Shirin. "One-pot low-temperature synthesis of high crystalline cu nanoparticles." Malaysian Journal of Science and Advanced Technology (2023): 122-127.